

RESEARCH

Recurrent Deep Embedding Networks for Genotype Clustering and Ethnicity Prediction

Md. Rezaul Karim^{1,2*†}, Michael Cochez^{1,2,4}, Oya Deniz Beyan², Achille Zappa³, Ratnesh Sahay³, Stefan Decker^{1,2} and Dietrich-Rebholz Schuhmann³

*Correspondence:

rezaul.karim@fit.fraunhofer.de

¹Fraunhofer FIT, Birlinghoven, Sankt Augustin, Germany

Full list of author information is available at the end of the article

†This manuscript has been prepared under the supervision of Prof. Dr. Stefan Decker and Prof. Dr. Dietrich Rebholz-Schuhmann.

Abstract

Background: a true understanding of genetic variations assists us in finding correlating population groups, identifying patients who are predisposed to common diseases and solving rare diseases. Albeit, machine learning algorithms have demonstrated tremendous success in this domain over the last decade but relatively less attention is paid in long-term dependencies and representations learning for classifying and clustering large and high-dimensional datasets. On the other hand, deep learning can better exploit such datasets to build networks that model non-linear relationships among millions of genetic variants. In this paper, we propose an improved variant of Deep Embedding Clustering (DEC) algorithm called Convolutional Deep Embedding Clustering (CDEC) for clustering genetic variants. Recurrent Long-short Term Memory (LSTM) on the other hand, is used for predicting geographic ethnicity from individual's sample.

Results: we used genotype data from the 1000 Genomes project covering genetic variants of 2504 individuals from 26 different ethnic origins, giving 84 million variants to train and evaluate the CDEC and LSTM networks. Experimental results show the efficiency and effectiveness of our approach. In particular, CDEC can cluster targeted population groups in 22 hours with an Adjusted Rand Index (ARI) of 0.915, a Normalized Mutual Information (NMI) of 0.92 and a Clustering Accuracy (ACC) of 0.89. LSTM network on the other hand, can predict the ethnicity of samples from unknown genetic variants with an accuracy of 95.6%, precision of 95%, recall of 93%, F1 of 93% and an RMSE of only 3.15%.

Conclusion: experimental results with a focus on accuracy and scalability outperforms state-of-the-art approaches with a high-level of clustering and classification accuracy. Overall, our approach is scalable for 5% to 100% of the full human genetic variants.

Keywords: Population Genomics; Genotype Clustering; Geographic Ethnicity; Convolutional Deep Embedding Clustering; Long-short Term Memory.

1 Introduction

Structural variants are implicated in numerous diseases and make up the majority of varying nucleotides among human genomes [1], which is one of the most important benefits of studying human genetic variation is the discovery and description of the genetic contribution to many human diseases [2].

Thus, a true understanding of genetic variations assists us in finding corresponding population groups from genetic variants and identifying patients who are predisposed to common diseases and solving rare diseases later on. This is an increasingly powerful motivation in light of our growing understanding of the contribution that

genes make to the development of diseases such as cancer, heart disease, and diabetes [2].

However, these potential uses of genomic information in biomedical practice require access to enough genomics data and efficient analytic methodologies to cope with such dataset consist of millions of genetic variants from thousands of individuals [3, 4, 5, 6]. The Next Generation Genome Sequencing (NGS) has made such dataset easily available by reducing overheads and time for genomic sequencing leading to the production of such genetic variants in an unprecedented way. The data sets provided by various genomics projects, such as The Cancer Genome Atlas (TCGA) [1], International Cancer Genome Consortium [2], 1000 Genomes Project, The Human Genome Project (HGP) [3], and Personal Genome Project(PGP) [4] etc. contributes large-scale data.

The HGP showed that important genetic differences exist between individuals. Inspired by HGP, the 1000 Genomes Project seeks to measure those differences to help medical researchers understand the roles of genetic variants in health and illness. Thus, one of the most important tasks is the analysis of genomic profiles to attribute individuals to specific ethnic populations or the analysis of nucleotide haplotypes for diseases susceptibility [7].

Subsequently, data from the 1000 Genomes project [1, 8] serves as one of the prime sources to analyze genome-wide single nucleotide polymorphisms (SNPs) at scale for predicting individual's ancestry with regards to continental and regional origins.

Research [9] also exposed that population groups from Asia, Europe, Africa, and America can be separated based on their genomic data. However, it is more challenging to accurately predict the haplogroup and the continent of origin, i.e. geography, ethnicity, and language. Another recent research [9] shows that the Y chromosome lineage can be geographically localized, forming the evidence for clustering the human alleles of the human genotypes. This signifies that clustering individual's genetic variants are correlated with geographic origin and ancestry.

Since the race depends on ancestry as well, corresponding clusters correlate with the traditional concepts of race. Unfortunately, this correlation is not perfect since genetic variation occurs according to probabilistic principles. Therefore, it does not follow any continuous distribution in different races rather overlaps across (or spills into) different populations.

As a result, an identification of ancestry, or even race, may prove to be useful for biomedical reasons. However, any direct assessment of disease-related genetic variation will ultimately yield more accurate and beneficial information [10].

Considering these motivations, in this paper, we will focus on the following research questions and try to answer in an accurate and scalable way: i) How are the human genetic variations distributed geographically i.e. among different population groups? ii) Can we use the genetic profile of individuals to attribute them to specific populations or derive from their nucleotide haplotype the disease susceptibility? iii) Is individual's genomic data suitable to predict geographic origin (i.e. the population group for an individual)?

[1] <https://cancergenome.nih.gov/> [2] <https://dcc.icgc.org/> [3] <http://humangenomes.org/>
[4] <http://www.personalgenomes.org/>

Unfortunately, answering to these question is very challenging since unprecedented increases in such data (i.e. in terms of a number of samples overall and features per sample) is computationally expensive and increasingly becomes the key bottleneck [11] by contrast. Consequently, these datasets also demand solutions for massively parallel data processing, which imposes extraordinary challenges to machine learning algorithms and bioinformatics approaches [11].

Albeit, machine learning algorithms are being in use in order to address above challenges by exploiting non-linear relationships between the genetic variants data, existing approaches still fail to model such relationship from very high-dimensional datasets (see Section 5).

To address this issue further, researchers come up with different improved variants of deep learning architectures that can be trained on the genomic data to classify or cluster the genomes of the populations.

In particular, a recurrent network such as LSTM is able to handle long sequences though recurrent hidden neurons. Since the current hidden state depends on the previous state and input of current time-step, each hidden neuron can accept preceding information. This way, LSTM can model contextual information dynamically.

On the other hand, unlike classical clustering algorithms (e.g. K-means), deep learning based clustering algorithms such as Deep Embedding Clustering (DEC) [12] can be used to refine clusters with an auxiliary target distribution derived from the current soft cluster assignment and gradually improves the clustering as well as the feature representation.

This way, deep learning based models can learn better feature representations so does perform mapping from data space to a lower-dimensional feature space well. Then cluster assignments can be done using Autoencoders, which iteratively optimizes the clustering objective.

Therefore, these deep architectures help us improve the quality of the training and overall learning for both classification and clustering tasks. Consequently, such trained model can be reused to infer the missing genotypes too.

In this paper, we try to address above questions and computational challenges in a scalable and efficient way. We first, applied Spark and ADAM for pre-processing large-scale and high-dimensional genetic variants data from the 1000 Genomes project. Then we examined how to improve state-of-the-art Deep Embedding Clustering (DEC) algorithm [12] aiming to cluster all the genetic variants at population scale (i.e. determining inter and intra-population groups).

We then performed the pre-training with the stacked convolutional autoencoder (SCAE) reconstruction loss (RL). Optimization is then done using both RL and cluster assignment hardening (CAH) loss jointly. We named this improved variant of DEC as Convolutional Deep Embedding Clustering (CDEC).

On the other hand, we train an LSTM network to more accurately predict the population group for an individual according to the individual's genomic data. apply

The rest of the paper is structured as follows: section 2 describes the motivation behind this work referring to the 1000 Genomes project dataset. Section 3 chronicles our proposed approach in detail with materials and methods. Section 4 demonstrates some experimental results, discuss the findings and highlights the limitations of the study. Section 5 discusses some related works with their emerging

use cases and potential limitations. Finally, section 6 provides some explanations of the importance and relevance of the study reported and discuss some future works before concluding the paper.

2 1000 Genomes Project: a Catalog of Human Genetic Variants

The data from the 1000 Genomes Project used in this study acts as a deep and large catalog of human genetic variants [8]. The project aims to determine genetic variants with frequencies above 1% in the populations studied.

2.1 Data collection

The 1000 Genomes project started in 2008 with a consortium consisting of more than 400 life scientists. Phase three of this project finished in September 2014 covering 2504 individuals from 26 populations (i.e. ethnical background) in total [13]. All the donars were healthy adults of aged 18 years and older.

Population samples were then grouped into 5 super-population groups according to their predominant ancestry. Each of the 26 populations has about 60-100 individuals from Europe, Africa, America and Asia.

- East Asian (EAS): CHB, JPT, CHS, CDX, and KHV
- European (EUR): CEU, TSI, FIN, GBR, and IBS
- African (AFR): YRI, LWK, GWD, MSL, ESN, ASW, and ACB
- American (AMR): MXL, PUR, CLM, and PEL
- South Asian (SAS): GIH, PJJ, BEB, STU and ITU.

2.2 Extracting genetic variants

Genomic data from every sample was combined to attribute all variants to a region. All individuals were then sequenced using both, whole-genome sequencings (mean depth = $7.4x$ [5]) and targeted exome sequencing (mean depth of $65.7x$).

In addition, individuals and their first-degree relatives such as adult offsprings were genotyped using high-density SNP microarrays – each genotype comprises all 23 chromosomes and a separate panel file [6] containing the sample and population information. Table 1 gives an overview of the different releases of the 1000 Genomes project.

Table 1: Statistics of the 1000 Genomes Project’s genotype dataset

1000 Genome release	Variants	Individuals	Populations	File format
Phase 3	84.4 million	2504	26	VCF
Phase 1	37.9 million	1092	14	VCF
Pilot	14.8 million	179	4	VCF

This way, about 88 million variants (84.7 million single nucleotide polymorphisms (SNPs), 3.6 million short insertions/deletions (indels), and 60 000 structural variants) have been identified as high-quality haplotypes [1, 8].

In short, 99.9% of the variants consist of SNPs and short indels. Less important variants – including SNPs, indels, deletions, complex short substitutions and other structural variant classes – have been removed for quality control, which leaves a total of 84.4 million variants.

[5] x is the number of average reads that are likely to be aligned at a given reference bp.

[6] ftp://ftp.1000genomes.ebi.ac.uk/vol1/ftp/release/20130502/integrated_call_samples_v3.20130502.ALL.panel

2.3 Data availability

The data is made openly available [7] in Variant Call Format (VCF)[8]. Then made freely accessible through public data repositories to scientists worldwide. Additionally, the data includes the population's region for each sample which is used for the predicted category in our approach.

Data from the 1000 Genomes project are widely used to screen variants discovered in exome data from individuals with genetic disorders and in cancer genome projects [1].

Specific chromosomal data (in VCF format) may have additional information denoting the super-population of the sample or the sequencing platform used. For multiallelic variants, each alternative allele frequency (AF) is presented in a comma-separated list shown in listing 1.

```
1 15211 rs78601809 T G 100 PASS AC=3050;AF=0.609026;
AN=5008;NS=2504;DP=32245;EAS_AF=0.504;AMR_AF=0.6772;
AFR_AF=0.5371;EUR_AF=0.7316;SAS_AF=0.6401;AA=t|||;VT=SNP
```

Listing 1: An example of multi allelic variants in 1000 Genomes project

**It is to be noted that the Allele Frequency (AF) is calculated as the quotient of Allele Count (AC) and Allele Number (AN) and NS is the total number of samples with data, where *_AF denotes the AF for a specific region. On the other hand, AF in the five super-population groups is calculated from allele numbers (range=[0,1]).

3 Materials and Methods

In this section, we describe our proposed approach in detail. First, we describe our feature engineering step we followed to get the training data consisting of feature vectors and labels. Then we chronicle the CDEC and LSTM networks constructions for clustering and classifying genetic variants of different population groups respectively. Finally, we describe the training process and hyper-parameter tuning.

3.1 Preprocessing and feature engineering

The large-scale data from release 3 of the 1000 Genomes project contributes to 770 GB of data. Since analyzing DNA and RNA sequencing data requires large-scale data processing to interpret the data according to its context, large-scale data processing solutions – such as ADAM-Spark – is used to achieve the scalable genomics data analytics platform with the support for the VCF file format so that we can transform genotype based RDD to Spark DataFrame.

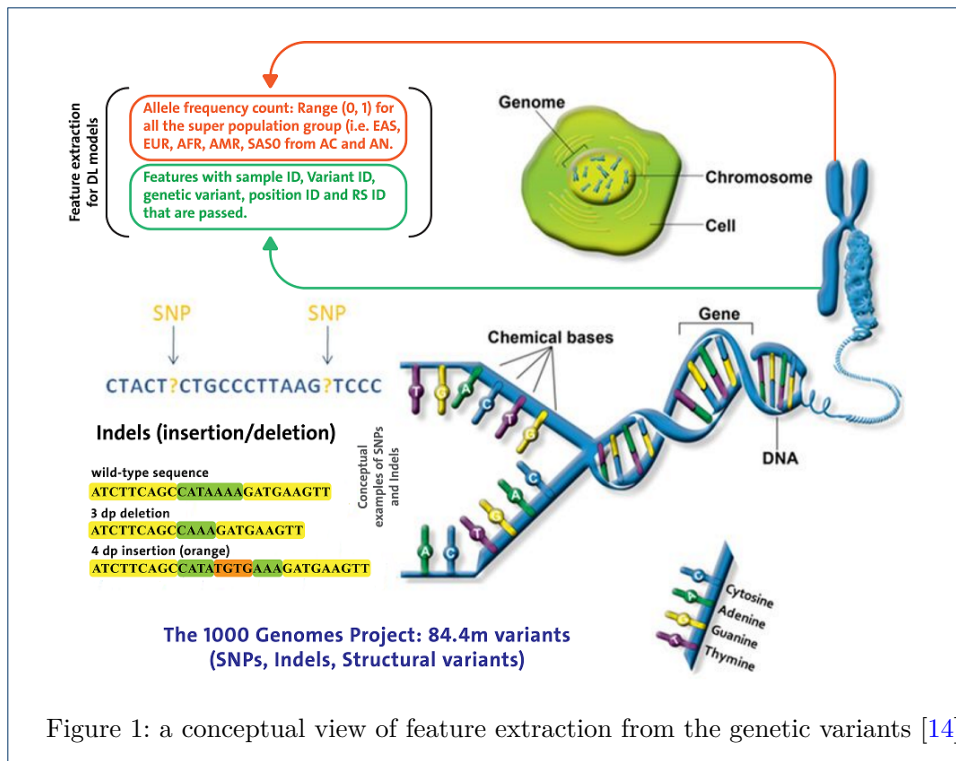
While Sparkling Water[9] transforms the data between ADAM and Spark. In short, ADAM and Spark are used to pre-process and prepare the input data (i.e. train, test, and validation set) to train Keras-based CDEC and LSTM networks in a faster and scalable way.

Since the genotypic information is required for the clustering and classification analysis, we prepared the features (containing the sample ID, variation ID and the

[7] <ftp://ftp.1000genomes.ebi.ac.uk/vol1/ftp/release/20130502/>

[8] <http://www.internationalgenome.org/wiki/Analysis/vcf4.0/>

[9] <https://www.h2o.ai/sparkling-water/>



count of the alternate alleles where the majority of variants that we used are SNPs and indels from each sample) as follows.

First, we process the panel file with Spark to extract only the targeted population data and identify the population groups. To be more specific, the panel file contains the sample ID of all individuals, population group, ethnicity, super population group, and the gender as shown in table 2.

Table 2: A snapshot from the Panel file from the 1000 Genomes Project

Sample ID	Pop Group	Ethnicity	Super pop. group	Gender
HG00096	GBR	British in England and Scotland	EUR	male
HG00171	FIN	Finnish in Finland	EUR	female
HG00472	CHS	Southern Han Chinese	EAS	male
HG00551	PUR	Puerto Ricans from Puerto Rico	AMR	female

The ADAM is then used to parse the genetic variants in VCF format, which generates an RDD^[10] of genotype data. Then another round of filtering is performed to extract only the relevant population groups, i.e. the data for individuals and the super population groups.

Then the filtered genotype object is converted into a Sample Variant object, which contains only the data we’re interested in such as sample ID, which uniquely identifies a particular sample, a variant ID, which uniquely identifies a particular genetic variant, and a count of alternate alleles (only when the sample differs from the reference genome).

Furthermore, since ADMIXTURE’s underlying statistical model does not take linkage disequilibrium (LD) into account, authors of literature [15] have suggested to remove all the variants with high LD for possible improvement in clustering

[10] Resilient Distributed Dataset

accuracy. Based on this suggestion, we not only remove all the variants having high LD but also all the incomplete variants in the preprocessing step (we further investigate its consequences in section 4).

The total number of samples (or individuals) has been determined, before grouping them using their variant IDs, and filtering out variants without support by the samples to simplify the data pre-processing and to better cope with the very large number of variants (in total 84.4 million). Figure 2 shows the overall processing pipeline of our proposed approach.

Then the frequency of all the alternate alleles is calculated for each variant and all the variants having less than 12 alternate alleles have been excluded leaving about 73 million variants in the analysis. Then from this large collection of variants, we finally acquired required features such as the sample ID, the variant ID for the genetic variants, position id, the RS id, and the count of alternate alleles.

Nevertheless, we group the variants by sample ID and sort them for each sample in a consistent manner using the variant IDs. Finally, this gives us a Spark DataFrame, where a row in the data matrix represents an individual sample and each column represents a specific variant. Whereas the "Region" refers as the class label (i.e., the *response column*). Eventually, this tabular data is in a very sparse vector representation to achieve better performance for the large number of variants when training the model (refer to literature [16] for details).

3.2 Ethnicity prediction using LSTM network

In this subsection, we discuss how we model the ethnicity prediction problem using LSTM network. Then we discuss the training procedure.

3.2.1 Network construction

Given genetic variants of an individual as an input sequence $x = x_1, x_2, \dots, x_T$, RNN computes its recurrent hidden state h_t and output vector y_t based on previous hidden state h_{t-1} and current input x_t as follows:

$$h_t = g(W h_{t-1} + U x_t) \quad (1)$$

$$y_t = f(V h_t) \quad (2)$$

where W , U and V correspond to the weight matrices between the current hidden state with previously hidden state, current input, and output respectively. The functions $g(\cdot)$ and $f(\cdot)$ are element-wise activation functions such as a logistic sigmoid function or hyperbolic tangent function.

However, this standard RNN can only exploit the preceding context but since current output may not only depend on previous context information but also succeeding context information. To address this issue, we attempted using bidirectional RNN (BRNN) to access both the preceding and succeeding contexts so that both the long-distance correlations among genetic variants with all the input history information can be tracked.

However, during the training phase, gradient parameters is found to be vanished or exploded exponentially in processing long sequences. This problem refrains us

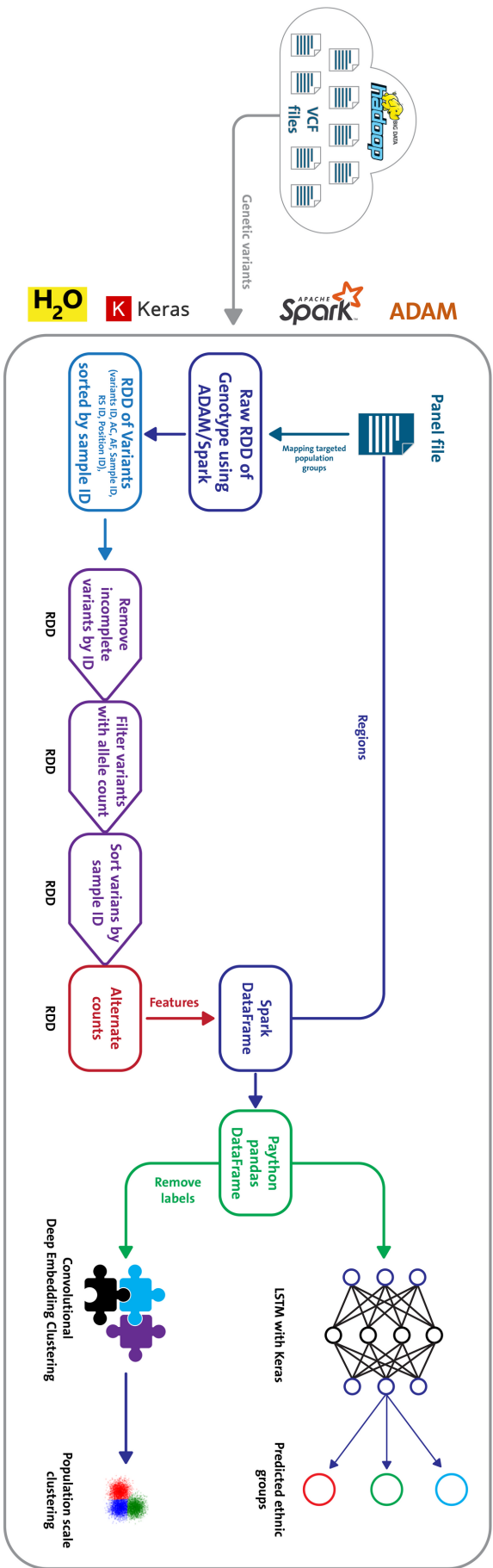
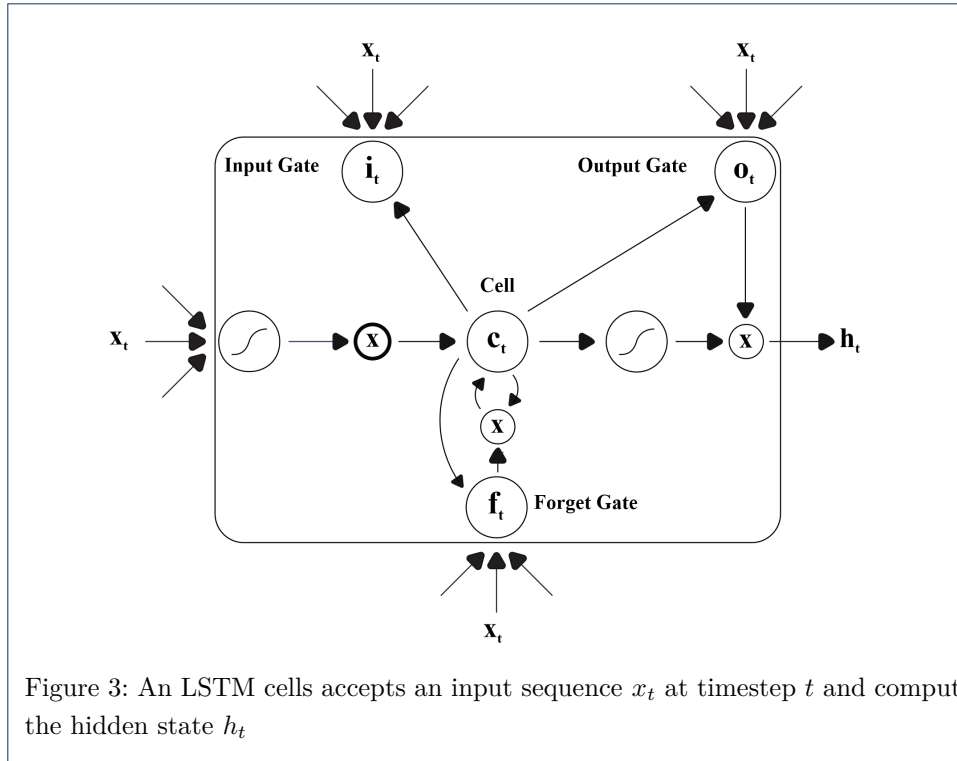


Figure 2: Pipeline of the presented approach (Color coding: color represents different/homogeneous objects, Pentagon: operation/action/input, Rounded rectangle: output, Arrow: output mapping)



from using BRNN to handle long-term dependencies to model the relationships between genetic variants for an individual as a sequence at each time-step.

To address this issue further, we investigated and found that another improved RNN variant called Long short-term memory (LSTM) can be used to deal with both gradient vanishing and exploding problem. In LSTM, all the hidden units of original RNN are replaced by memory blocks, where each memory block contains a memory cell to store input history information and three gates to define how to update the information. These gates are input gate, forget gate and output gate as outlined in fig. 3.

This way, LSTM can learn long-distance correlations among genetic variants with all the input history information, which is important for handling sequence data. Then for given genetic variants of an individual can be used as an input sequence $x=x_1, x_2, \dots, x_T$. Which further help us compute the modified hidden state h_t as follows:

$$i_t = \sigma(W_i x_t + U_i h_{t-1} + V_i c_{t-1}) \quad (3)$$

$$f_t = \sigma(W_f x_t + U_f h_{t-1} + V_f c_{t-1}) \quad (4)$$

$$O_t = \sigma(W_o x_t + U_o h_{t-1} + V_o c_{t-1}) \quad (5)$$

$$O_t = \sigma(W_o x_t + U_o h_{t-1} + V_o c_{t-1}) \quad (6)$$

$$\tilde{c}_t = \tanh(W_c x_t + U_c h_{t-1}) \quad (7)$$

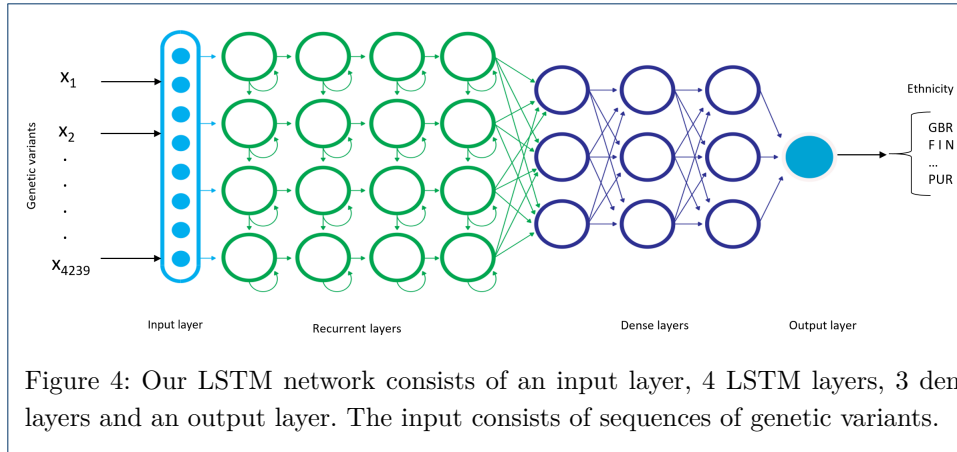


Figure 4: Our LSTM network consists of an input layer, 4 LSTM layers, 3 dense layers and an output layer. The input consists of sequences of genetic variants.

$$c_t = f_t^i \odot c_{t-1} + i_t \odot \tilde{c}_t \quad (8)$$

$$h_t = \tanh(c_t) \quad (9)$$

where c_t stands for a memory cell, i denotes an input gate to control how much new input formation is added to the memory cell, f is a forget gate to control how much existing memory is forgotten, and o is the output gate to control the amount of memory content exposure. The entries of the gating vectors (i.e. i_t , f_t , o_t) lie within the range of $[0, 1]$.

Whereas $\sigma(\cdot)$ and $\tanh(\cdot)$ are sigmoid and hyperbolic tangent activation function respectively. The symbol \odot denotes element-wise multiplication. This way, LSTM has enabled us in modeling and learning long-term dependencies overlong sequence consisting of genetic variants.

3.2.2 Network training

Before we start training the LSTM network outlined in fig. 4, we convert the Spark DataFrame into sequence format so that it can be feed into LSTM network. Further, we randomly split the sequence data into train, test and validation sets with 60%, 20%, and 20% ratio for the training, testing and validation purposes respectively.

Assuming the training data consist of p population groups then for each group x_i , we have a set $Y(x_i)$ of actual group prediction and a set $G(x_i)$ of predicted population groups generated by the LSTM network.

Therefore, if the set of labels or class of the populations groups is given as $L = \{\ell_0, \ell_1, \dots, \ell_{M-1}\}$, then the true output vector y will be have N elements such that $\mathbf{y}_0, \mathbf{y}_1, \dots, \mathbf{y}_{N-1} \in L$.

We then start training the LSTM network, which takes only one sequence at each time-step and generates a prediction vector by minimizing the cross-entropy of the true versus predicted distributions $\hat{\mathbf{y}}$ of N elements such that $\hat{\mathbf{y}}_0, \hat{\mathbf{y}}_1, \dots, \hat{\mathbf{y}}_{N-1} \in L$. When training the network, keeping the test set separate from the validation set enables us to learn hyper-parameters for the model as suggested in [17].

We use ADADELTA adaptive learning rate algorithm [18] that automatically combines the benefits of learning rate annealing and momentum training to avoid slow convergence of the LSTM network. The ReLU activation function is used in

the LSTM layers for the better regularization and a drop out probability was set to a high value (i.e. 0.9 in our case) to avoid possible overfitting.

In the output layer, Softmax activation function is used for the probability distribution over the classes. This enables us computing the elements of the confusion matrix for our multiclass classification problem as follows:

$$C_{ij} = \sum_{k=0}^{N-1} \hat{\delta}(\mathbf{y}_k - \ell_i) \cdot \hat{\delta}(\hat{\mathbf{y}}_k - \ell_j) \quad (10)$$

where the delta function $\hat{\delta}(x)$ can be defined as follows:

$$\hat{\delta}(x) = \begin{cases} 1 & \text{if } x = 0, \\ 0 & \text{otherwise} \end{cases} \quad (11)$$

Then the confusion matrix formulated in eq. (10) can be reused to compute performance metrics such as weighted precision, weighted recall and weighted f1 measure of the predicted population labels against the true population labels using the following formulas^[11]:

$$Precision_w = PPV_w = \frac{1}{N} \sum_{\ell \in L} PPV(\ell) \cdot \sum_{i=0}^{N-1} \hat{\delta}(\mathbf{y}_i - \ell) \quad (12)$$

$$Recall_w = TPR_w = \frac{1}{N} \sum_{\ell \in L} TPR(\ell) \cdot \sum_{i=0}^{N-1} \hat{\delta}(\mathbf{y}_i - \ell) \quad (13)$$

$$F1_w = F_w(\beta) = \frac{1}{N} \sum_{\ell \in L} F(\beta, \ell) \cdot \sum_{i=0}^{N-1} \hat{\delta}(\mathbf{y}_i - \ell) \quad (14)$$

where $PPV(\ell)$, $TPR(\ell)$ and $F(\beta, \ell)$ are the precision, recall and F1 by labels. Furthermore, we computed the root means square error (RMSE) using eq. (15) of the network errors.

$$RMSE = \sqrt{\frac{\sum_{i=0}^{N-1} (\mathbf{y}_i - \hat{\mathbf{y}}_i)^2}{N}} \quad (15)$$

Furthermore, we applied grid-searching technique with 10-fold cross validation for finding the best hyperparameters. Moreover, to improve the classification results, we applied batch normalization, kept the adaptive rate, and force load balance for replicating the entire training dataset onto every node for faster training.

Finally, when the training is completed, trained model is used to score against test set to measure predicted population groups versus genetic variants producing a confusion matrix for the performance in a multiclass setting using eq. (10).

3.3 Genotype clustering using Convolutional Deep Embedded Clustering network

Albeit, K-means clustering algorithm and its several variants have been proposed to address issues with higher-dimensional input spaces, they are fundamentally limited to linear embedding. Hence, cannot model non-linear relationships [19]. Nevertheless, fine-tuning in these approaches are based on only cluster assignment hardening loss. Therefore, a fine-grained clustering accuracy cannot be achieved.

[11] <https://spark.apache.org/docs/latest/mllib-evaluation-metrics.html>

Further, genetic variants data does not come like other numeric or categorical data, hence non-linear embedding is necessary for such a complex dataset and state-of-the-art approaches such as DEC [12] and DBC [20] comes as saviors. Our approach is mostly based on DEC but we perform the training in two phases:

- Pretraining with a convolutional autoencoder (CAE) reconstruction loss (RL)
- Optimizing CAE’s RL and K-means’s cluster assignment hardening (CAH) loss jointly.

In other words, the parameter optimization that gets iterated between computing an auxiliary target distribution and minimizing the Kullback–Leibler (KL) divergence [21] optimizing both reconstruction and cluster assignment hardening (CAH) losses jointly to it.

Therefore, the second phase is different from both DEC, which omit the reconstruction loss and use only the CAH loss. However, a recent research [22] suggest that omitting reconstruction loss during the second phase could lead to worse representations and solutions. Therefore, combining both RL and CAH loss is more reasonable (see fig. 5).

Let’s consider our unlabeled data consists of a set of n data points $\{\mu_j \in X\}_{i=1}^n$ (where $i = 1 \dots n$ represent genetic variants) features into k clusters (i.e. k population groups), each represented by a centroid $\mu_j, j = 1 \dots k$ [12].

Then in order to avoid the “curse of dimensionality”, we transform the data with a nonlinear mapping function $f_\theta: X \rightarrow Z$, where θ are learnable parameters and Z is the latent feature space having much smaller dimensionality compared to X . This way, deep architectures are perfect fit to parametrize f_θ .

Then similar to DEC, we also cluster the data points by learning a set of k cluster centers $\{\mu_j \in Z\}_{j=1}^k$ in the feature space Z and the parameters of the deep network that maps data points into Z simultaneously.

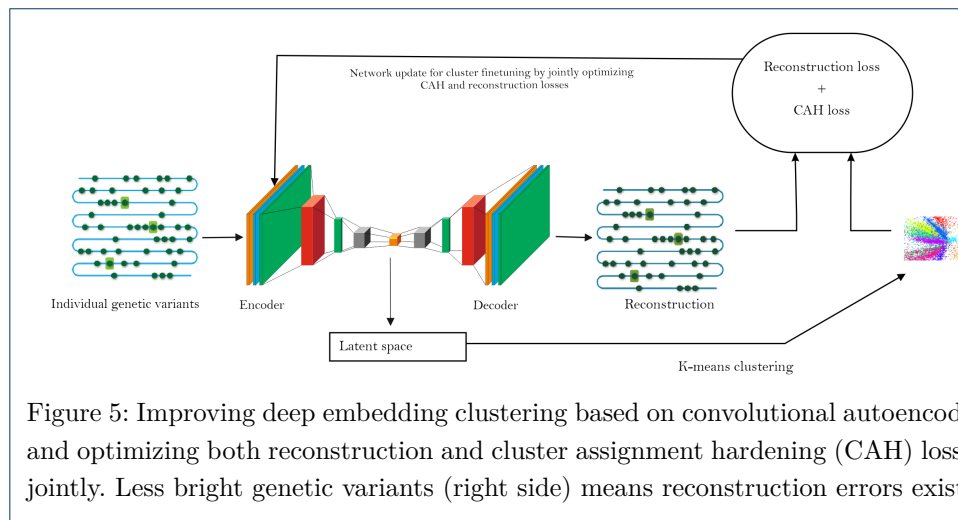


Figure 5: Improving deep embedding clustering based on convolutional autoencoder and optimizing both reconstruction and cluster assignment hardening (CAH) losses jointly. Less bright genetic variants (right side) means reconstruction errors exist.

3.3.1 Clustering genetic variants with KL divergence

Given an initial estimate of the non-linear mapping f_θ and the initial cluster centroids $\{\mu_j\}_{j=1}^k$, CDEC performs clustering in an unsupervised way (similar to [12])

that alternates between two steps. In the first step, CDEC computes the soft assignment between the embedded points and the cluster centroids.

The second step updates the deep mapping f_θ and refines the cluster centroids by learning from current high confidence assignments using an auxiliary target distribution. This process is repeated until a convergence criterion is met. We used student's t-distribution[23] as a kernel to measure the similarity between embedded point z_j and centroid μ_j (similar to literature [12]) as follows:

$$q_{ij} = \frac{(1 + \|z_i - \mu_j\|^2/\alpha)^{-\frac{\alpha+1}{2}}}{\sum_{j'} (1 + \|z_i - \mu_{j'}\|^2/\alpha)^{-\frac{\alpha+1}{2}}} \quad (16)$$

where $z_i = f_\theta(x_i) \in Z$ corresponds to $x_i \in X$ after embedding, α is the degrees of freedom of the Student's t-distribution and q_{ij} is the probability of assigning sample i to cluster j (i.e. soft assignment).

Then CDEC refines the clusters by learning from their high confidence assignments with the help of an auxiliary target distribution so that the model is trained by matching the soft assignment to the target distribution. This is the objective definition as a KL divergence loss between the soft assignments q_i and the auxiliary distribution p_i as follows:

$$L = \text{KL}(P||Q) = \sum_i \sum_j p_{ij} \log \frac{p_{ij}}{q_{ij}} \quad (17)$$

Since setting the target distributions P is crucial for deep learning based clustering performance, we adopted similar technique proposed in literature [12]: we compute p_i by raising q_i to the second power and then normalizing by frequency per cluster as follows:

$$p_{ij} = \frac{q_{ij}^2/f_j}{\sum_{j'} q_{ij'}^2/f_{j'}} \quad (18)$$

where $f_j = \sum_i q_{ij}$ are soft cluster frequencies. Once, the KL divergence gets minimized, the next task that we did is optimizing the cluster centers $\{\mu_j\}$ and θ using Stochastic Gradient Descent (SGD) with momentum [24]. Then the gradients of L with respect to feature-space embedding of each data point z_i and each cluster centroid μ_j are computed as:

$$\frac{\partial L}{\partial z_i} = \frac{\alpha + 1}{\alpha} \sum_j \left(1 + \frac{\|z_i - \mu_j\|^2}{\alpha}\right)^{-1} \quad (19)$$

$$\begin{aligned} & \times (p_{ij} - q_{ij})(z_i - \mu_j) \\ \frac{\partial L}{\partial \mu_j} &= -\frac{\alpha + 1}{\alpha} \sum_i \left(1 + \frac{\|z_i - \mu_j\|^2}{\alpha}\right)^{-1} \quad (20) \\ & \times (p_{ij} - q_{ij})(z_i - \mu_j) \end{aligned}$$

The gradients $\partial L/\partial z_i$ are then used in standard backpropagation to compute the network's parameter gradient $\partial L/\partial \theta$. This iterative process continues until less than tol% of points change cluster assignment between two consecutive iterations for discovering cluster assignments.

3.3.2 Parameter initialization

Unlike literature [12], we initialize the network using Stacked Convolutional Autoencoder (SCAE) layer by layer. Here each layer being a convolutional autoencoder trained to reconstruct the previous layer's output after random corruption, which is a two layer network that can be mathematically formulated as follows:

$$\tilde{x} \sim \text{Dropout}(x) \quad (21)$$

$$h = g_1(W_1\tilde{x} + b_1) \quad (22)$$

$$\tilde{h} \sim \text{Dropout}(h) \quad (23)$$

$$y = g_2(W_2\tilde{h} + b_2) \quad (24)$$

where $\text{Dropout}(\cdot)$ [25] is the dropout operation, g_1 and g_2 are activation functions for encoding and decoding layer respectively, and $\theta = \{W_1, b_1, W_2, b_2\}$ are model hyperparameters parameters.

A greedy layer-wise training is performed by minimizing the least-squares loss $\|x - y\|_2^2$. That is after training one layer, we use its output h as the input to the next layer and so on. We use rectified linear units (ReLUs) as activation function in all encoder and decoder pairs, except for g_2 of the first pair and g_1 of the last pair.

Once this greedy layer-wise training is finished, we concatenate all the encoder and decoder layers in reverse layer-wise training order, to form a deep autoencoder and then finetune it to minimize reconstruction loss. The final result is a multilayer deep convolutional autoencoder with a bottleneck coding layer in the middle.

Then both the encoder and decoder layers are used as the initial mapping between the data space and the feature space. Finally, to initialize the cluster centers, the data is passed through the initialized network to get embedded data points. Then the standard k-means is applied in the feature space Z to obtain k initial centroids $\{\mu_j \in Z\}_{j=1}^k$. Then we feedback both the CAH and reconstruction losses to further fine-tune the clustering.

3.3.3 Network training

First, we removed the labels before training the CDEC. Then we normalize the data so that $\frac{1}{d}\|x_i\|_2^2$ is approximately 1, where d is the dimensionality of the data space point $\{x_i \in Z\}$. We then set network dimensions to *in*-5000-2500-1000-*out* for our dataset, where *in* is 4239 is the data-space dimension and *out* is the number of predicted population groups, having 5,000 unit in both encoder and decoder layer and layers are fully connected.

During the greedy layer-wise pre-training, we initialize the network weights using Xavier [26] and each layer is pretrained for 100,000 iterations with a dropout rate of 50%. The entire deep convolutional autoencoder is then finetuned for 100,000 iterations without dropout.

For both layer-wise pretraining and end-to-end finetuning of the autoencoder, minibatch size is set to 128, starting learning rate is set to 0.01 to make the training more exhaustive, which is divided by 10 every 10,000 iterations, and weight decay is set to 0. Nevertheless, in the KL divergence minimization phase, we train with a constant learning rate of 0.01 with a convergence threshold of $tol = 0.1\%$.

Since performing cross-validation was not a viable option with this network setting, these parameters are set naively but still, gives reasonably low reconstruction loss. To initialize the centroids, we iterate k-means for 100 times (since apart from k , k-means does not have any other tunable hyperparameters) and select the best k value.

Nevertheless, we took the advantage of three methods: Elbow [27], generalizability G and Normalized Mutual Information (NMI) for determining the optimal number of clusters to be set prior building the K-means model. Initially, we thought setting up the number of clusters to the number of ground-truth categories and evaluate performance with unsupervised clustering [12]. However, this is less efficient for empirical methods like Elbow.

Thus, we stick with Elbow: we calculated the cost using Within-cluster Sum of Squares ($WCSS$) as a function of the number of clusters (i.e. k) for K-means algorithm applied to genotype data based on all the features from 26 population groups. Nonetheless, since Elbow performs better in a classical clustering setting, for evaluating clustering results with different cluster number, NMI [12] is used, which can be formalized as follows:

$$NMI(l, c) = \frac{I(l, c)}{\frac{1}{2}[H(l) + H(c)]} \quad (25)$$

,where I is the mutual information metric and H is then entropy. Then G [12] is defined as the ratio between training and validation loss as follows:

$$G = \frac{L_{train}}{L_{validation}} \quad (26)$$

where G is small when training loss is lower than validation loss, which indicates a high degree of overfitting.

Nevertheless, a good clustering performance is also characterized by high intra-cluster similarity and low inter-cluster similarity for the data points. Therefore, we used the Rand index (RI) which measures the percentage of decisions that are correct to evaluate the clustering quality. The RI was normalized to Adjusted Rand Index (ARI) for values between -1 (independent labeling) and 1 (perfect match) [28].

This way, the adjusted metric exhibits some random variations centered on a mean score of 0.0 for any number of samples and clusters. Therefore, only an adjusted measure can hence safely be used as a consensus index to evaluate the average stability of clustering algorithms for a given value of k on various overlapping sub-samples of the dataset. The following formula is used to calculate the ARI (other state-of-the-art approaches such as VariationSpark [15] and ADMIXTURE [29] also used this metric):

$$RI = \frac{TP + TN}{TP + FP + FN + TN} \quad (27)$$

Finally, to evaluate the clustering quality in unsupervised way, clustering accuracy (ACC) [12] metric is calculated as follows:

$$ACC = \max_m \frac{\sum_{i=1}^n 1\{l_i = m(c_i)\}}{n} \quad (28)$$

where l_i is the ground-truth label and c_i is the cluster assignment produced by the algorithm whereas m ranges over all possible one-to-one mappings between clusters and labels. ACC takes a cluster assignment from an unsupervised algorithm and a ground truth assignment and then finds the best matching between them.

4 Experiments and Results

In this section, we discuss the evaluation results both quantitatively and qualitatively. Furthermore, a comparative analysis between the state-of-the-art and our approach will be provided in the end.

4.1 Experimental setup

The proof of the concept of our approach is implemented in Spark, ADAM, and Keras. In particular, for the scalable and faster preprocessing of huge number of genetic variants across all the chromosomes (i.e. 820GB of data), we used ADAM and Spark to convert the genetic variants from VCF format to Spark DataFrame. Then we convert Spark DataFrame into NumPy arrays. Finally, we use Keras to implement LSTM and CDEC networks.

Experiments were carried out on a computing cluster (having 32 cores, 64-bit Ubuntu 14.04 OS). Software stack consisting of Apache Spark v2.3.0, H2O v3.14.0.1, Sparkling Water v1.2.5, ADAM v0.22.0 and Keras v2.0.9 with TensorFlow backend. It is to be noted that we used this low number of cores to compare the capability of our approach with the state-of-the-art such as ADMIXTURE [3] and Variation-Spark [30].

A modified version of Keras based DEC implementation [12] proposed by Ali F. et al. [31] is used in our approach. Network training were carried out on a Nvidia TitanX GPU with CUDA and cuDNN enabled to make the overall pipeline faster.

4.2 Ethnicity classification analysis

When the training is completed, our trained LSTM network is used for inferencing that scored against the test set to measure the predicted population groups versus genetic variants. For the demonstration purpose, we extracted genetic variants of only 5 population groups from chromosome 22 genetic variants (having 494,328 allele) allowing 5 class and compare the true labels to the same number of predicted ethnicity labels (i.e. 'ASW', 'CHB', 'CLM', 'FIN', 'GBR').

Even this random sample selection gives a good classification accuracy (i.e. 95.09%) as a confusion matrix as shown in Table 3. Furthermore, for the full dataset (with all the genetic variants) and with the above experiment setting, our LSTM network can classify the whole population groups with a precision of 94%, a recall of 93% and an F1 measure of 93.50%. We experienced an RMSE of 3.15% which is much better than that of [17].

The reason for this improvement is that LSTM network was less confused between predicted classes compared to other deep networks such as MLP or DBN one in literature [17]. Nevertheless, since all the variants with high LD and incomplete variants were removed in the preprocessing step, this has contributed towards a better classification accuracy. The reason is simple— with that minor factor, we removed some impurities.

[12] <https://github.com/XifengGuo/DEC-keras>

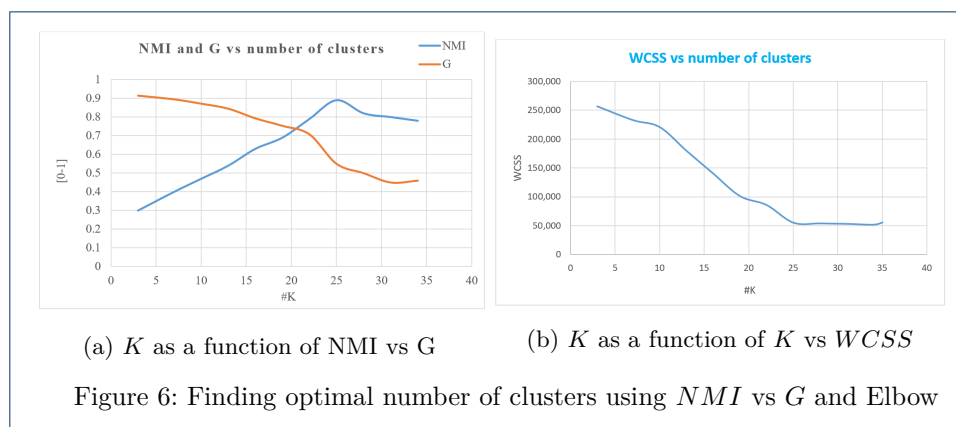
Table 3: Confusion matrix from LSTM classifier (vertical: actual; across: predicted)

Group	ASW	CHB	CLM	FIN	GBR	Error	Support
ASW	59	0	1	1	0	0.0328	2/61
CHB	0	103	0	0	0	0.0000	0/103
CLM	3	0	86	3	2	0.0851	8/94
FIN	0	0	86	3	2	0.0202	2/99
GBR	0	0	1	9	81	0.1099	10/91
Total	62	103	174	16	85	0.0491	22/448

4.3 Genotype scale clustering analysis

Before showing the effectiveness of our approach, we first, investigated if our CDEC converges to the optimal number of population groups. We start the training by setting $K = 2$ and increased up to 35 and see how CDEC performs the clustering operation.

The finding of optimal number of K can be perceived in fig. 5a, which plots NMI and G vs. number of clusters. The graph clearly shows that there is a sharp drop of generalizability from 26 to 27 which means that 26 is the optimal number of clusters and to further support this argument, the graph also shows that for 26, we observed the highest NMI of about 0.92.



Then we focused on investigating how the K-means converged during the cluster assignment hardening and training. For this, we utilized Elbow method. During the training we calculated the cost metric called Within-cluster Sum of Squares ($WCSS$) as a function of the number of clusters (i.e. k). From fig. 5b, we can observe a drastic fall of $WCSS$ value when number of cluster was around 25 and 26.

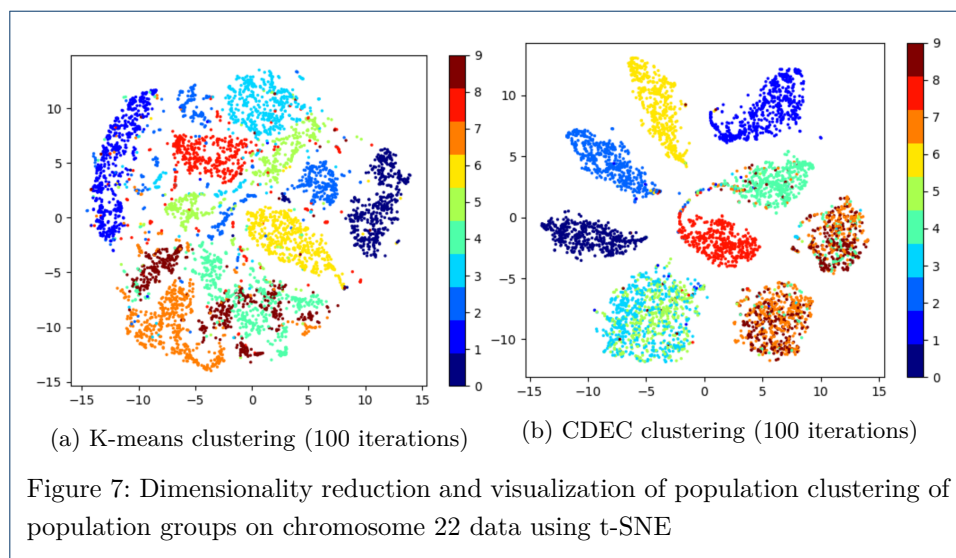
Based on this optimal K and with the above experiment setting, CDEC successfully completes clustering of the whole dataset in 22 hours with an ARI of 0.915, an NMI of 0.92 and Clustering Accuracy (CA) of 0.89 as outlined in table 4.

Table 4: Clustering result comparison^[13]

Approach	ARI	NMI	ACC	Time	Data Size	Algorithm
CDEC	0.915	0.92	0.89	22h	770GB	CDEC
VariantSpark	0.82	N/A	N/A	30h	770GB	K-means
ADMIXTURE	0.25	N/A	N/A	35h	770GB	Maximum likelihood

VariationSpark on the other hand, requires 30h to finish the overall computation and leverage an ARI of 0.82. On the other hand, ADMIXTURE performs clustering based on the maximum likelihood estimation (MLE) of individual ancestries from

multi-locus SNP genotype datasets and takes considerably high time of about 35h giving an ARI of only 0.25 [30].



One potential reason behind this low clustering accuracy is MLE-based approaches are limited in their ability to accurately estimate the population mean and standard deviation [32] for the 1000 Genomes project dataset.

For the demonstration purpose, we further cluster the individuals from chromosome 22 (having with 494,328 allele) allowing 10 clusters and compare the assigned labels to the same number of reported ethnicity labels (i.e. ‘GBR’, ‘FIN’, ‘CHS’, ‘CLM’, ‘PUR’, ‘IBS’, ‘PEL’, ‘CDX’, ‘ACB’, ‘GWD’). This random selection even provided very good clustering compared to the K-means one as shown in tSNE graph in fig. 7.

Furthermore, to compare our approach with VariationSpark, we also investigate the cluster quality for 5 super-population groups (i.e. EUR, AMR, AFR, EAS, SAS) for each individual to the label assigned by CDEC-based clustering. For this experiment, we use both ARI, ACC and NMI metrics, which resultant an ARI of 0.87, a ACC of 0.86 and an NMI of 0.88. This signifies that our approach has higher accuracy (at least in terms of ARI).

However, this is still low compared to our overall ARI. The reason for such clustering accuracy and quality is that the genotypes data from African (AFR), East Asian (EAS), and American (AMR) super population groups are relatively homogeneous. Nevertheless, similar to literature [30], European (EUR) and South Asian (SAS) are more mixed so didn’t cluster well. Moreover, EUR is more mixed and consists predominantly of individuals.

Finally, we investigate which super-population group contains what percentage of human genetic variants. This study gives an interesting statistics showing that majority of the genotype variants were clustered into EUR (28.32%) and lowest into AMR (12.68%). On the other hand, the distribution for EAS, AFR, and SAS found were 22.25%, 18.65% and 18.10% respectively.

4.4 Discussion

Our approach can perform clustering on VCF files from 2504 individuals consist of 84 million variants in just 22h allowing faster clustering for well-characterized cohorts where 20% of the genome is sufficient for the training. Our approach uses ADAM and Spark for allowing in-memory caching and hence 32% and 90% faster compared to VariantSpark and ADMIXTURE respectively.

It has also been observed [33] that it is quite hard to get an MLP with more than three layers to work well on some data sets such as very high-dimensional numeric (or even image) classification problems, even when pre-training with a DBN. Therefore, we stick with LSTM network to deal with long length sequences consisting of high-dimensional genetic variants while applying classification.

While using CDEC, it gives us an opportunity to pretrain the model using a standard input reconstruction loss function. The clustering operation is then fine-tuned using cluster assignment hardening loss and the clustering centers are updated accordingly. As a result, our clustering method showed better result compared to the state-of-the-art.

5 Related Work

The 1000 Genomes Project Consortium developed a global reference for human genetic variation for exome and genome sequencing. Later on, biological sequence alignment in distributed computing system as [34] is an example of using Spark for genome sequence analysis.

Lek M. et al. [35], described the aggregation and analysis of high-quality protein-coding region and DNA sequence data for 60,706 individuals of diverse ancestries. They calculated the objective metrics of pathogenicity for sequence variants and identified genes subject to strong selection against various classes of mutation.

They have been able to identify as much as 3,230 genes with near-complete depletion of predicted protein-truncating variants, while 72% of these genes have no currently established human disease phenotype. It has also been demonstrated that these data can be used for the efficient filtering of candidate disease-causing variants, and for the discovery of human 'knockout' variants in protein-coding genes.

One of the commonly used tools is ADMIXTURE [29], which performs maximum likelihood estimation of individual ancestries from multilocus SNP genotype datasets. However, this approach cannot cluster genetic variants comfortably, with an ARI of only 0.25. Finally, ADMIXTURE also requires a pre-processing step from VCF to PED format, which is pretty time-consuming.

To address the shortcomings of ADMIXTURE, VariantSpark was proposed by Aidan R. et al. [30], which provides an interface from MLib to the standard variant format (VCF) that offers a seamless genome-wide sampling of variants and provides a pipeline for visualizing results from the 1000 Genomes Project and Personal Genome Project (PGP). However, overall clustering accuracy is rather low and VariantSpark does not provide any support for classifying individuals based on the genotypic information.

Thus to overcome these issues, in our previous work [17], we applied H2O based K-means with fine-tuning for the population scale clustering and achieved better accuracy. For the classification tasks, we applied H2O-based an MLP classification algorithm that achieved a state-of-the-art classification result.

However, two limitations still remained: i) The feature extraction process was based on SPARQL queries which took a long time for the whole chromosome dataset. Moreover, genotype datasets needed to be converted into Resource Description Format (RDF) [11] which also took a non-trivial amount of effort. ii) Good performance was obtained for the genotype dataset for a single chromosome due to a low number of latent variables, but for the whole chromosome data, poor results were obtained because of the overfitting issue and the lack of generalization in the training phase.

6 Conclusion and Outlook

In this paper, our Spark and ADAM based data processing is particularly suitable for handling large-scale genomic dataset. Our LSTM model can predict geographic ethnicity successfully and is consistent with all the genotypic dataset consisting of all the chromosomes.

On the other hand, our CDEC clustering approach can cluster a set of data points consisting of genetic variants in a jointly optimized feature space, which can be viewed as an unsupervised extension of semi-supervised self-training. Similar to [12], our CDEC clustering solution also has linear complexity with respect to a number of data points, this allowed us to scale to large datasets (i.e. 770GB).

Nevertheless, a recent research [35] has shown that the apparent separation between East Asian and other samples reflects a deficiency of Middle Eastern and Central Asian samples in the dataset. It is found that European individuals can be separated into persons of Finnish and non-Finnish ancestry.

Therefore, in future, we intend to provide a more detailed analysis on intra-superpopulation groups and discuss the homogeneity and heterogeneity among different groups. Secondly, we would like to extend this work by considering other datasets (e.g. PGP) and factors like predicting population groups within larger geographic continents.

Finally, it would be worth exploring whether we can make share representations of the features from both 1000 Genomes project and PGP datasets and cluster them simultaneously using CDEC.

Availability of data and materials

Source codes and some supplementary materials will be made publicly available soon on GitHub at <https://github.com/rezacsedu/VariationDEC>. The 1000 Genomes project dataset was downloaded from <http://www.internationalgenome.org/data> and used in our study.

Funding

This publication has emanated from research conducted with the financial support of Science Foundation Ireland (SFI) under the Grant Number SFI/12/RC/2289. Part of the work was performed at the Fraunhofer Institute for Applied Information Technology FIT, Germany.

Author's contributions

MRK implemented the algorithms and drafted the manuscript. MC drafted the manuscript and carried out the classification and clustering analysis. ODB carried out the studies of the 1000 Genomes Project. AZ participated in proofreading and performed the statistical analysis. SD and DRS conceived of the study, and participated in its design and coordination and helped to draft the manuscript. All authors read and approved the final manuscript.

Acknowledgments

This article is based on a workshop paper discussed at the Extended Semantic Web Conference (ESWC'2017) Workshop on Semantic Web Solutions for Large-scale Biomedical Data Analytics (SeWeBMeDA), in Slovenia, May 28-29, 2017. The authors would like to thank the anonymous reviewers for their useful comments which helped us to further extend and improve the draft and come up with this manuscript.

Author details

¹Fraunhofer FIT, Birlinghoven, Sankt Augustin, Germany. ²Chair of Computer Science 5 - Information Systems, RWTH Aachen University, Aachen, Germany. ³Insight Centre for Data Analytics, National University of Ireland Galway, IDA Business Park, Dangan Lower, Co. Galway, Ireland. ⁴Faculty of Information Technology, University of Jyväskylä, Jyväskylä, Finland.

References

1. Consortium, .G.P., *et al.*: An integrated map of genetic variation from 1,092 human genomes. *Nature* **491**(7422), 56 (2012)
2. Miller, M.P., Kumar, S.: Understanding human disease mutations through the use of interspecific genetic variation. *Human molecular genetics* **10**(21), 2319–2328 (2001)
3. Alexander, D.H., Novembre, J., Lange, K.: Fast model-based estimation of ancestry in unrelated individuals. *Genome research* **19**(9), 1655–1664 (2009)
4. Gao, X., Starmer, J.: Human population structure detection via multilocus genotype clustering. *BMC genetics* **8**(1), 34 (2007)
5. Padhukasahasram, B.: Inferring ancestry from population genomic data and its applications. *Frontiers in genetics* **5** (2014)
6. Kidd, J.M., Gravel, S., Byrnes, J., Moreno-Estrada, A., Musharoff, S., Bryc, K., Degenhardt, J.D., Brisbin, A., Sheth, V., Chen, R., *et al.*: Population genetic inference from personal genome data: impact of ancestry and admixture on human genomic variation. *The American Journal of Human Genetics* **91**(4), 660–671 (2012)
7. Laitman, Y., Feng, B.-J., Zamir, I.M., Weitzel, J.N., Duncan, P., Port, D., Thirthagiri, E., Teo, S.-H., Evans, G., Latif, A., *et al.*: Haplotype analysis of the 185delag brca1 mutation in ethnically diverse populations. *European Journal of Human Genetics* **21**(2), 212 (2013)
8. Consortium, .G.P., *et al.*: A global reference for human genetic variation. *Nature* **526**(7571), 68 (2015)
9. Zoë H. Rosser, M.E.H.e.a. Tatiana Zerjal: Y-chromosomal diversity in europe is clinal and influenced primarily by geography, rather than by language. *The American Journal of Human Genetics* **67**(6), 1526–1543 (2000). doi:[10.1086/316890](https://doi.org/10.1086/316890)
10. Jorde, L.B., Wooding, S.P.: Genetic variation, classification and race. *Nature genetics* **36**, 28–33 (2004)
11. Karim, M.R., Michel, A., Zappa, A., Baranov, P., Sahay, R., Rebholz-Schuhmann, D.: Improving data workflow systems with cloud services and use of open data for bioinformatics research. *Briefings in Bioinformatics*, 039 (2017)
12. Xie, J., Girshick, R., Farhadi, A.: Unsupervised deep embedding for clustering analysis. In: *International Conference on Machine Learning*, pp. 478–487 (2016)
13. Birney, E., Soranzo, N.: Human genomics: The end of the start for population sequencing. *Nature* **526**(7571), 52–53 (2015)
14. Karim, M.R.: *Scala Machine Learning Projects*. Packt Publishing Ltd. (2018)
15. O'Brien, A.R., Saunders, N.F., Guo, Y., Buske, F.A., Scott, R.J., Bauer, D.C.: Variantspark: population scale clustering of genotype information. *BMC genomics* **16**(1), 1052 (2015)
16. Bottou, L., Curtis, F.E., Nocedal, J.: Optimization methods for large-scale machine learning. *arXiv preprint arXiv:1606.04838* (2016)
17. Karim, M.R., Zappa, A., Sahay, R., Rebholz-Schuhmann, D.: A deep learning approach to genomics data for population scale clustering and ethnicity prediction, 1–15 (2017)
18. Zeiler, M.D.: ADADELTA: an adaptive learning rate method. *CoRR abs/1212.5701* (2012)
19. Aggarwal, C.C., Reddy, C.K.: *Data Clustering: Algorithms and Applications*, pp. 1–350. CRC press, ??? (2014)
20. Li, F., Qiao, H., Zhang, B., Xi, X.: Discriminatively boosted image clustering with fully convolutional auto-encoders. *arXiv preprint arXiv:1703.07980* (2017)
21. Hershey, J.R., Olsen, P.A.: Approximating the kullback leibler divergence between gaussian mixture models. In: *Acoustics, Speech and Signal Processing, 2007. ICASSP 2007. IEEE International Conference On*, vol. 4, p. 371 (2007). IEEE
22. Aljalbout, E., Golkov, V., Siddiqui, Y., Cremers, D.: Clustering with deep learning: Taxonomy and new methods. *arXiv preprint arXiv:1801.07648* (2018)
23. Maaten, L.v.d., Hinton, G.: Visualizing data using t-sne. *Journal of machine learning research* **9**(Nov), 2579–2605 (2008)
24. Sutskever, I., Martens, J., Dahl, G., Hinton, G.: On the importance of initialization and momentum in deep learning. In: *International Conference on Machine Learning*, pp. 1139–1147 (2013)
25. Srivastava, N., Hinton, G., Krizhevsky, A., Sutskever, I., Salakhutdinov, R.: Dropout: A simple way to prevent neural networks from overfitting. *The Journal of Machine Learning Research* **15**(1), 1929–1958 (2014)
26. Glorot, X., Bengio, Y.: Understanding the difficulty of training deep feedforward neural networks. In: *Proceedings of the 13th International Conf. on Artificial Intelligence and Statistics*, pp. 249–256 (2010)
27. Tibshirani, R., Walther, G., Hastie, T.: Estimating the number of clusters in a data set via the gap statistic. *Journal of the Royal Statistical Society: Series B (Statistical Methodology)* **63**(2), 411–423 (2001)
28. Santos, J.M., Embrechts, M.: On the use of the adjusted rand index as a metric for evaluating supervised classification. In: *International Conference on Artificial Neural Networks*, pp. 175–184 (2009). Springer
29. Parra, E.J., Marcini, A., Akey, J., Martinson, J., Batzer, M.A., Cooper, R., Forrester, T., Allison, D.B., Deka, R., Ferrell, R.E., *et al.*: Estimating african american admixture proportions by use of population-specific alleles. *The American Journal of Human Genetics* **63**(6), 1839–1851 (1998)
30. O'Brien, A.R., Saunders, N.F., Guo, Y., Buske, F.A., Scott, R.J., Bauer, D.C.: Variantspark: population scale clustering of genotype information. *BMC genomics* **16**(1), 1052 (2015)
31. Alexander, D.H., Novembre, J., Lange, K.: Unsupervised deep embedding for clustering analysis **48** (2016)
32. Jain, R.B., Wang, R.Y.: Limitations of maximum likelihood estimation procedures when a majority of the observations are below the limit of detection. *Analytical chemistry* **80**(12), 4767–4772 (2008)

33. Hinton, G.E., *et al.*: Modeling pixel means and covariances using factorized third-order boltzmann machines. In: *Computer Vision and Pattern Recognition (CVPR), 2010 IEEE Conference On*, pp. 2551–2558 (2010). IEEE
34. Massie, M., Nothaft, F., Hartl, C., Kozanitis, C., Schumacher, A., Joseph, A.D., Patterson, D.A.: Adam: Genomics formats and processing patterns for cloud scale computing. EECS Department, University of California, Berkeley, Tech. Rep. UCB/EECS-2013-207 (2013)
35. Lek, M., Karczewski, K., Minikel, E., Samocha, K., Banks, E., Fennell, e.a.: Analysis of protein-coding genetic variation in 60,706 humans. *BioRxiv*, 030338 (2016)